Fire Technology

Manufactured in The United States
https://doi.org/10.1007/s10694-022-01217-2

# The Effect of Surrounding Water on the Burning Rates of Pool Fires

*Vinay C. Raj and Harshad Shrigondekar, Department of Mechanical Engineering, Indian Institute of Technology, Powai, Mumbai 400 076, India*
*Bhaskar Dixit, Centre for Disaster Mitigation, Jain University, Bangalore, India*
*H. S. Mukunda, Combustion Gasification and Propulsion Laboratory, Indian Institute of Science, Bangalore, India*
*S. V. Prabhu*, Department of Mechanical Engineering, Indian Institute of Technology, Powai, Mumbai 400 076, India*

**Received:** 22 July 2021/**Accepted:** 3 February 2022

***Abstract.*** The present paper investigates the effect of water surrounding the pan on the characteristics of an open pool fire. Experiments conducted on 2 m square pool fires surrounded by water indicated lower values for mass burning rate, adiabatic surface temperature, and heat flux. It was hypothesized that this decrease is due to the interaction between the pool fire and the water surrounding it. To test this hypothesis, experiments are conducted on a 0.5 m diesel pool fire with and without water surrounding the pan. For the case of water surrounding the pool fire, the mass burning rate decreased by 32% and the temperatures are found to be lower by approximately 100 °C in the core region of the pool fire when compared with experiments with no water surrounding the pool fire. The entrainment of water in the form of vapors, from the water surrounding the pan, into the fire results in a decrease in temperature and also changes the dynamics of the pool. This results in a decrease in the net heat feedback and hence the mass burning rate. The decrease in the mass of the surrounding water and the observation of boiling on its surface, support the claim. It is inferred that there is a decrease in the total heat flux to the cask in a pool fire that is surrounded by water. Thus, it is advisable that the pool fire testing of nuclear casks be carried out by ensuring no interaction between the pool fire and the water surrounding it.

**Keywords:** Mass loss rate, Temperature, Heat flux, Diesel pool fire, And surrounding water

**Nomenclature**

| | |
|---|---|
| $C_p$ | Specific heat ($J/Kg\ K$) |
| $D$ | Pool diameter ($m$) |
| $d$ | Thermocouple bead diameter ($m$) |
| $h$ | Heat transfer coefficient ($W/m^2K$) |
| $k$ | Thermal conductivity ($W/mK$) |
| $\dot{m}''$ | Mass loss rate ($g/m^2s$) |

*Correspondence should be addressed to: S. V. Prabhu, E-mail: svprabhu@iitb.ac.in

Published online: 28 February 2022

| | |
|---|---|
| $\dot{q}''$ | Heat flux ($W/m^2$) |
| $T$ | Temperature ($K$) |
| $V$ | Velocity ($m/s$) |
| $\Delta h_g$ | Heat of gasification ($J/Kg$) |
| $t$ | Time (s) |

**Greek Symbols**

| | |
|---|---|
| $\rho$ | Density ($kg/m^3$) |
| $\varepsilon$ | Emissivity (-) |
| $\delta$ | Thickness ($m$) |
| $\kappa$ | Extinction coefficient ($m^{-1}$) |
| $\beta$ | Mean beam length corrector (-) |
| $\mu$ | Dynamic Viscosity ($Pa\text{-}s$) |
| $\sigma$ | Stefan-Boltzmann constant ($5.67 \times 10^{-8}\ W/m^2\ K^4$) |

**Subscript**

| | |
|---|---|
| $\infty$ | Infinite pool diameter |
| $AST$ | Adiabatic surface temperature |
| $Conv$ | Convective |
| $eq$ | Equivalent |
| $f$ | Flame |
| $loss$ | Loss in the form of wall conduction |
| $PT$ | Plate thermometer |
| $rad$ | Radiative |
| $rr$ | Re-radiation |
| $TC$ | Thermocouple |

**Non-dimensional numbers**

| | |
|---|---|
| $\mathrm{Pr} = \frac{\mu C_p}{k}$ | Prandtl number |
| $\mathrm{Re} = \frac{\rho V D}{\mu}$ | Reynolds number |

# 1. Introduction

Accidental fires involving nuclear casks are a major concern to society as they can cause health risks due to possible radiation leakage. Nuclear packages have to undergo extensive pool fire tests before they are certified as per the transport regulations of the International Atomic Energy Agency (IAEA) [1]. The safety standards of IAEA requires a 30-min exposure of the test specimen to a thermal environment which provides a heat flux at least equivalent to that of a hydrocarbon fuel/air fire with a minimum emissivity of 0.9, an average temperature of 800 °C, fully engulfing the specimen with an absorptivity of 0.8 or a value that the package may have demonstrated. These tests are intended to simulate a fully engulfing pool fire scenario occurring in case of a transportation accident involving spillage of large quantities of hydrocarbon fuels.

Over the last few decades, comprehensive testing facilities have been developed by Sandia National Laboratories for testing and certification of radioactive material packages [2]. Complete guidelines for planning, conducting, and reporting

thermal tests on transport packages for radioactive materials have been compiled by VanSant et al. [3]. For performing thermal tests, cylindrical casks filled with insulating material are used to simulate real transportation packages. Temperature distributions inside the cask are generally obtained through thermocouples. The heat flux onto the cask from the pool fire is then determined by using inverse heat conduction codes such as the Sandia one-dimensional direct and inverse thermal (SODDIT) and one-dimensional inverse heat conduction problem (IHCP-1D) [4–7].

Various researchers have reported experiments on the characterization of packages in pool fires. Kramer et al. [6] performed experiments to measure the heat transfer to a completely engulfed cylindrical calorimeter in a large-scale JP-8 pool fire. The spatial and temporal variations of temperature and heat flux of the calorimeter were determined. Logenbaugh et al. [7] studied the thermal response of a 0.46 m diameter vertically oriented cask in a pool fire of 1.8 m diameter. The thermal response of the cask (surface temperature and incident heat flux) to three different thermal environments with test duration of 100 min was investigated. Koski et al. [8] determined the thermal response of a water-cooled vertical calorimeter in a 6 × 6 m outdoor and 3 × 3 m indoor JP-4 pool fires.

Gregory et al. [9] performed a series of large-scale pool fire tests to obtain information about the thermal exposure to calorimeters. Temperature and heat flux data were obtained for the core region of the pool fire. They reported a peak heat flux of 100–160 kW/m$^2$ and articulated that the heat flux distribution is contradictory to the distribution predicted by simplified radiation models that assume uniform flame temperatures. A series of three fire tests were performed at the Sandia National Laboratories by del Valle et al. [10] wherein a large calorimeter, 2.4 m in diameter and 4.6 m in length was suspended above a 7.2 m diameter JP-8 pool fire. A computer code CAFE (The Container Analysis Fire Environment) was used to simulate the test results with the measured wind velocity applied as a boundary condition. Despite the difference in fuel evaporation rates, the simulations were capable of accurately predicting the average temperature rise of the calorimeter.

The thermal response of bodies engulfed in di-tert-butyl peroxide pool fires is studied numerically by Sudheer et al. [11]. Large-scale methane gas burner experiments and liquid methane pool fire experiments on the water have been conducted in Sandia National Laboratories by Luketa and Blanchat [12]. The pool fire experiments of diameter 21 m and 56 m were conducted to improve the hazard predictions by obtaining measurements of flame height, smoke production, and mass burning rate. They reported that LNG pool fires on water display different behavior than those on land by producing less smoke. Essentially, pool fire testing of nuclear packages is carried out with the fuel floating on water in a container of a specific dimension so that the pool fire completely engulfs the cask [13]. The water provides a flat surface and ensures the fuel is completely burnt. The test facility is sometimes surrounded by water to ensure the stability of the container [6, 13].

In the present paper, the authors carried out experiments to characterize the thermal response of cask in a 2 m square pool fire. A concrete pool consisting of

an outer chamber of dimension 4 × 4 × 1 m depth and an inner chamber of dimension 2 × 2 × 1 m depth was created as per ASTM specification [13] as shown in Fig. 1a. The inner and outer chambers are inter-connected through an opening in the inner chamber and are filled with water. The liquid pool is formed by floating a layer (100 mm) of diesel on water-filled in the inner chamber. To obtain the heat flux distribution, plate thermometers were attached to the cask as shown in Fig. 1b. The temperature and heat flux distribution obtained from plate thermometers attached to the cask was lower than expected. This leads to a hypothesis that the lower values of temperature and heat flux distribution obtained might be due to the interaction between the pool fire and the surrounding water, which can change the dynamics of a pool fire.

A comprehensive literature review indicated that studies on the effect of water surrounding the pan on the characteristics of pool fire have not been reported. The present work is thus aimed at investigating this effect by carrying out a series of experiments on small-scale diesel pool fires of diameter 0.5 m and measuring the mass burning rate and temperature distribution. The three different cases considered are:

a. Simple pool fire experiment with no water surrounding the pan
b. The second set of experiments is performed with water surrounding the pan. For this, a pan of diameter 0.5 m containing diesel is kept inside the second pan of diameter 0.7 m containing water.
c. The third set of experiments are performed by covering the open surface of the 0.7 m pan, containing water, with asbestos and an insulator (cerablanc) to avoid any interaction between fire and water.

Experiments are also conducted on a 2 m square diesel pool fire with no water surrounding the pan to determine the actual mass burning rate. These studies indicate that the water surrounding the pan has a profound influence on the mass burning rate of the pool fire, the adiabatic surface temperature, and heat flux onto the cask.

## 2. Experimental Procedure

All pool fire experiments are conducted in an open space to allow natural airflow into the fire. The wind velocity was monitored using a vane anemometer with the velocity being predominantly between 0.5 to 1 m/s. The fuel temperature and the ambient air temperature were at 33 °C and the relative humidity was reported to be about 60 to 70%.

To determine the thermal response of casks in a 2 m square diesel pool fire as a case for nuclear cask testing, experiments are carried out at the open pool fire test facility located in Jain University, Bengaluru, India. Figure 1a shows the schematic of the experimental setup for a 2 m square pool fire. An SS304L pipe is used to simulate the nuclear cask. Plate thermometers are used to determine the heat transfer to the cask. A plate thermometer is a plate made of Inconel having

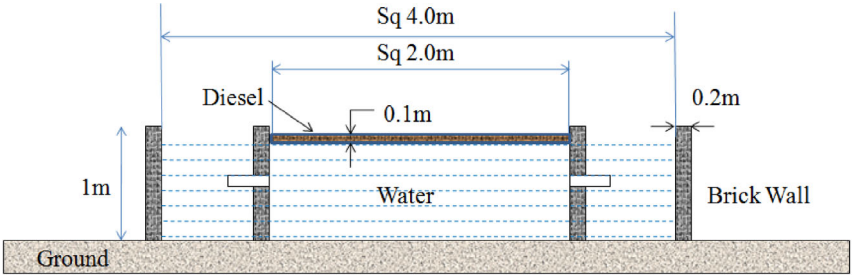


**(a) 2 m square pool fire surrounded by water**

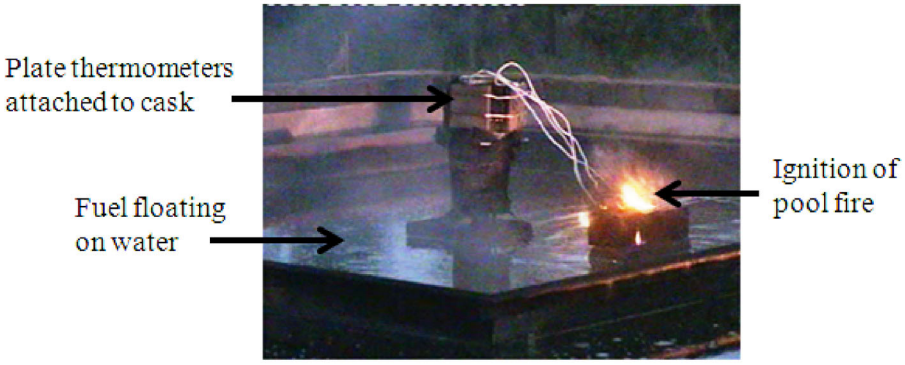


**(b) Cask with plate thermometers**

**Figure 1. Schematic of the experimental setup of pool fire pan surrounded by water.**

dimensions of 100 × 100 mm and 0.7 mm thick, with an insulating material (cerablanc) on one side. A thermocouple of 0.7 mm bead diameter is welded at the center. To eliminate any dependence of the measured temperature on the emissivity of the plate, the plate thermometer is painted with high-temperature paint (Pyromark flat black). Nakos and Keltner [14] and Logenbaugh et al. [7] have measured the emissivity of pyromark painted surface and reported that the emissivity is 0.86 ± 0.09 in the temperature range of 30–1200°C.

Four such plate thermometers, with their backsides insulated using cerablanc, are arranged at a 90° angle along the periphery of the SS304L pipe as shown in Fig. 1b. The plate thermometer assembly is supported using a stand made up of mild steel completely insulated using cerablanc. The cask is located at a distance of 0.4*D* from the base of the pool fire. This location is chosen for two particular reasons: (a) temperature of pool fire in this region is the highest [15] (b) most of the packages undergoing pool fire tests are located in this region [16]. The transient rise in the temperature of the flame is also captured using a thermal camera at every 1 s and the 80 images corresponding to the steady state is averaged.

To test the hypothesis and establish the effect of water surrounding the pool fire, small-scale pool fire experiments are carried out at IIT Bombay, Mumbai, India. The 0.5 m diameter pan made of mild steel has a depth of 5 cm and a thickness of 2 mm. The 0.7 m pan has a depth of 10 cm. Diesel is used as fuel and is filled to the brim. A 250 kg platform scale is used to measure the mass-loss rate of the pool fire. The accuracy of the platform scale is 0.02 kg. The weighing scale is thermally insulated from the pan and the fire through the asbestos sheet and cerablanc. The platform scale is interfaced with a computer through an RS232 port and the data is transferred every 0.5 s.

For the pool fire experiments with water surrounding the pan, the 0.5 m pan is kept inside the 0.7 m pan. The pans are arranged in such a way that the lips of the pans are on the same plane. Diesel is filled in a 0.5 m pan while water is filled in a 0.7 m pan. The water surrounds the 0.5 m pan from all the sides and also from the bottom as shown in Fig. 2.

To measure the temperature distribution in the 0.5 m diameter diesel pool fire, a K-type thermocouple tree with a bead of diameter 0.7 mm is used. The thermocouples are bare bead thermocouples inserted through a 30 cm long stainless steel tube with a ceramic insulator. A set of ten thermocouples are placed at a distance of 0.125 m along the centerline of the pool fire as shown in Fig. 2. Another set of five thermocouples are placed in water to determine the temperature rise in water. Four of these thermocouples (TC_2w to TC_5w) are located at a depth of 7.5 cm from the surface while one thermocouple (TC_1w) is placed at 2 cm from the surface. All the thermocouples are connected to a computer via Agilent data logger and the data is acquired at a sampling rate of 1 Hz. The transient temperature of the flame is measured using thermal camera similar to that for 2 m pool fire.

## 3. Data Reduction

### 3.1. Emissivity from Mass Burning Rate

Babrauskas [17] applied energy balance at the surface of the pool fire and obtained

$$\dot{m}''\Delta h_g = \dot{q}''_{rad} + \dot{q}''_{conv} + \dot{q}''_{rr} + \dot{q}''_{loss} \tag{1}$$

where $\dot{m}''$ is the mass-loss rate per unit area, $\Delta h_g$ is the total heat of gasification, and $\dot{q}''_{rad}$ is the radiant flux absorbed by the liquid pool. Losses in the form of wall conduction $\dot{q}''_{loss}$ and re-radiation $\dot{q}''_{rr}$ are usually small (less than 10%) and hence can be neglected. For radiatively dominant pool fires, heat received by convection $\dot{q}''_{conv}$ can also be neglected [17]. Thus,

$$\dot{m}'' = \frac{\dot{q}''_{rad}}{\Delta h_g} = \frac{\sigma \varepsilon_f T_f^4}{\Delta h_g} \tag{2}$$

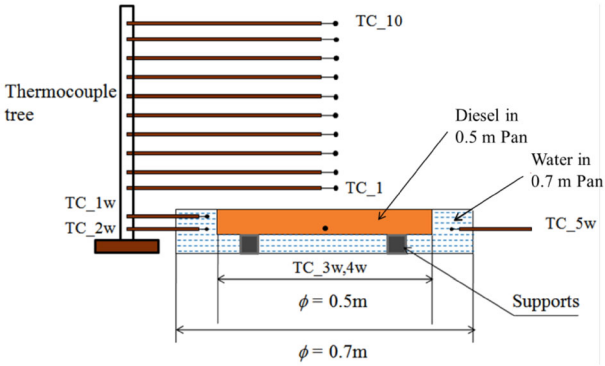


**Figure 2. Pool fire of 0.5 m diameter surrounded by water.**

For a pool fire of very large diameter (say > 4 m) the flame emissivity can be assumed to be equal to unity.

$$\dot{m}''_{\infty} = \frac{\sigma T_f^4}{\Delta h_g} \Rightarrow \frac{\dot{m}''}{\dot{m}''_{\infty}} = \frac{\frac{\sigma \varepsilon_f T_f^4}{\Delta h_g}}{\frac{\sigma T_f^4}{\Delta h_g}} = \varepsilon_f \tag{3}$$

Thus the overall emissivity of the flame can be determined by obtaining the ratio of the mass burning rate of a particular diameter to the mass burning rate of a pool fire of infinite diameter.

### *3.2. Adiabatic Surface Temperature*

Heat transfer to plate thermometers inside the fire depends on both radiation and convection boundary conditions. Wickstrom [18] suggested that in fire situations when the flame temperature is not uniform and the gas temperature and the effective radiation temperature are not equal, the fire temperature may be replaced by a characteristic temperature called the adiabatic surface temperature. The Adiabatic Surface Temperature (AST) can be defined as the temperature of a surface that neither absorbs nor loses heat to the environment. It is thus a weighted mean temperature of the radiation and convection component of the pool fire [18].

From the temperature measured using plate thermometers, the adiabatic surface temperature can be determined using Eq. (4) [16]:

$$\rho \delta C_p \frac{dT_{PT}}{dt} = \sigma \varepsilon_{PT} \left( T_{AST}^4 - T_{PT}^4 \right) + h(T_{AST} - T_{PT}) \tag{4}$$

$$\rho \delta C_p \frac{T_{PT}^{i+1} - T_{PT}^i}{\Delta t} = \sigma \varepsilon_{PT} \left[ \left( T_{AST}^i \right)^4 - \left( T_{PT}^i \right)^4 \right] + h\left( T_{AST}^i - T_{PT}^i \right) \tag{5}$$

where $\rho$: Density of the plate thermometer ($kg/m^3$), $\delta$: Thickness of the plate thermometer ($m$), $C_p$: Specific heat capacity ($kJ/kg.K$), $\sigma$: Stefan Boltzmann constant ($5.67 \text{ X } 10^{-8}$ $W/m^2K^4$), $\varepsilon_{PT}$: Emissivity of plate thermometer, $T_{AST}$: Adiabatic surface temperature ($K$), $T_{PT}$: Plate thermometer temperature ($K$), $h$: convective heat transfer coefficient ($W/m^2K$).

The assumption made in Eq. (4) is that the conduction heat loss to the insulation and the.

thermal inertia of the insulation are negligible. $T_{AST}$ is determined using the finite difference method as shown in Eq. (5). AST allows for the use of a simple boundary condition instead of the mixed radiation and convection boundary conditions for numerically modeling the heat flux onto the cask.

### 3.3. Radiation Correction of Temperature Measured using Thermocouple

Measurement of temperature using thermocouples is not representative of the true gas temperature. The temperature indicated by the thermocouple is lower than that of the gas because of the radiative loss from the thermocouple junction to the colder surroundings. Temperature correction for a thermocouple placed inside a flame front is provided by Silvani and Morandini [19] as shown in Eq. (6) and Eq. (7). Radiation correction for thermocouple measurements is a difficult process. Various parameters such as the thermocouple bead diameter, its emissivity, and the local gas properties like heat transfer coefficient, emissivity, and temperature influences the radiation correction.

$$T_f = T_{TC} + \frac{\sigma \varepsilon_{TC}\left(1-\varepsilon_f\right) T_f^4}{h + 4\sigma\varepsilon_{TC} T_f^3} \tag{6}$$

$$h = \frac{k_f}{d_{TC}}\left(0.43 + 0.53\mathrm{Re}^{0.5}\,\mathrm{Pr}^{0.31}\right) \tag{7}$$

$$\begin{aligned} \mathrm{Re} &= \frac{\rho V d_{TC}}{\mu} \\ \mathrm{Pr} &= \frac{\mu C_p}{\kappa} \end{aligned} \tag{8}$$

Due to the uncertainties in various parameters, the values that maximize the radiation errors are used [19]. The temperatures obtained from the thermocouple are corrected for radiation losses by taking emissivity of the bead ($\varepsilon_{TC}$) equal to 0.8 as soot gets deposited on it [19]. The heat transfer coefficient in Eq. (6) is obtained as flow over a cylinder from the Nusselt number correlation provided by Bergman et al. [20]. The bead diameter ($d_{TC}$) is measured to be equal to 0.7 mm. $k_f$, $\mu$, $\rho$, $C_p$ are the thermal conductivity, dynamic viscosity, density, and specific heat capacity of dry air at the thermocouple temperature ($T_{TC}$) for the first iteration.

For the subsequent calculations, these values are updated for the flame temperature ($T_f$). Velocity for calculation of Reynolds number is taken to be a constant of 1.5 m/s [16]. Substituting these values into the above set of equations with an initial guess for the flame temperature and iterating till convergence, the flame temperature is determined.

The uncertainty in the determination of flame temperature is calculated with the method suggested by Moffat [21]. An uncertainty of 6% or 70 K is obtained for the maximum temperature of 1200 K. A sensitivity analysis has been performed by varying the constants like emissivity of the thermocouple ($\varepsilon_{TC}$: $0.8 \pm 0.2$) and the velocity of the flame (1–3 m/s). The difference in the obtained flame temperature is around 10 K.

## 4. Results and Discussion

### *4.1. m Square Diesel Pool Fire*

Experiments are conducted on a 2 m square diesel pool fire to characterize the thermal response of the miniaturized cask. The cask is a SS304L pipe filled with an insulating material, Cerablanc. Mass burning rate and temperature distribution for the 2 m square pool fire is obtained. Adiabatic surface temperature and heat flux onto the cask is determined by using the four plate thermometers attached along the periphery of the cask.

*4.1.1. Mass Burning Rate of 2 m Square Diesel Pool Fire Surrounded by Water* The fuel is ignited at the edge of the pool using a flame torch. The flame rapidly spreads across the surface of the pool and within minutes completely engulfs the cask. The transient or the instantaneous mass burning rate of the pool fire is not determined. However, the fuel is completely burnt in 30 min. The overall mass burning rate is then calculated to be equivalent to 35 g/m$^2$s. Table 1 provides the average mass burning rate for the 2 m square diesel pool fire surrounded by water. Using Eq. (3), emissivity is determined to be equal to 0.65.

Babrauskas [17] provided an equation to determine the expected mass burning rate based on the mass burning rate of pool fire of very large diameter and the optical thickness of the flame.

$$\begin{aligned} \frac{\dot{m}''}{\dot{m}''_{\infty}} &= \varepsilon_f \\ \varepsilon_f &= 1 - e^{-\kappa\beta D} \\ \dot{m}'' &= \dot{m}''_{\infty}\left(1 - e^{-\kappa\beta D}\right) \end{aligned} \tag{9}$$

The mean beam length corrector extinction coefficient product for diesel pool fire is provided by Sudheer and Prabhu [15].

$$\kappa\beta = 1.16\, m^{-1} \tag{10}$$

**Table 1**
**Mass Loss Rate of Diesel Pool Fire**

| Sl no: | Experimental condition | Mass loss rate g/s | Mass loss rate g/m$^2$s | Average g/m$^2$s | Emissivity $\varepsilon_f = \frac{\dot{m}''}{\dot{m}''_\infty}$ |
|---|---|---|---|---|---|
| 1 | 2 m Square Pool fire surrounded by water | 136 | 34 | 35 | 0.65 |
| | | 144 | 36 | | |
| 2 | 2 m Square Pool fire not surrounded by water | 198 | 49.5 | 49.5 | 0.92 |
| 3 | 0.5 m pool Fire | 5.38 | 27.4 | 28.57 | 0.53 |
| | | 6 | 30.55 | | |
| | | 5.45 | 27.78 | | |
| 4 | 0.5 m Pool fire surrounded by water | 3.71 | 18.92 | 19.24 | 0.36 |
| | | 4 | 20.4 | | |
| | | 3.65 | 18.4 | | |
| 5 | 0.5 m Pool fire surrounded by water but covered with Asbestos | 5.74 | 29.22 | 28.73 | 0.53 |
| | | 5.65 | 28.78 | | |
| | | 5.54 | 28.21 | | |

The mass-loss rate of diesel pool fire of infinite diameter is provided by [22] and [24]

$$\dot{m}''_\infty = 54\, g/m^2 s \tag{11}$$

The equivalent circular pool diameter for a 2 m square pool fire is obtained.

$$D_{eq} = 2.26\text{m} \tag{12}$$

Thus, the expected mass burning rate of a 2 m square pool fire is

$$\dot{m}'' = 54(1 - e^{-1.16X2.26}) = 50.06 g/m^2 s \tag{13}$$

Similarly, the expected mass burning rate of a 0.5 m pool fire is

$$\dot{m}'' = 54(1 - e^{-1.16X2.26}) = 23.77/m^2 s \tag{14}$$

*4.1.2. Temperature Distribution* Figure 3 shows the instantaneous temperature distribution of a 2 m square diesel pool fire. The temperature distribution is obtained by setting the emissivity value equal to 0.97 as an input to the thermal camera. It has been shown that for pool fires of diameter greater than about 2 m, the emissivity value of 0.97 can be used [23]. The origin for Fig. 3 is chosen at the center of the base of the pool and the horizontal and the vertical axis are non-dimensionalized by dividing the axis with the equivalent diameter of the pool fire. The temperature distribution indicates a core region of 1100 K and the temperature

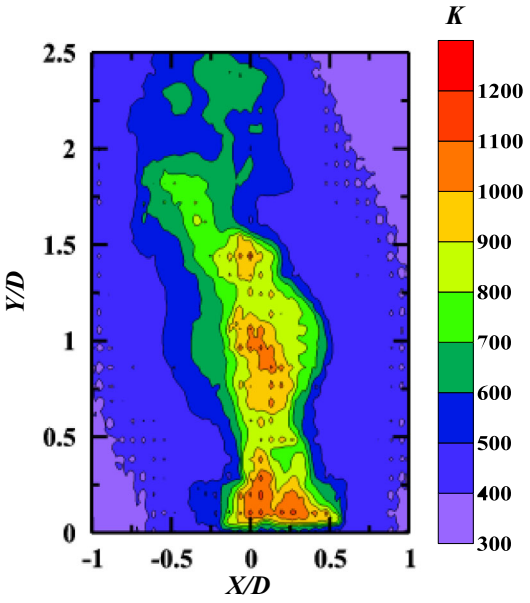


**Figure 3. Instantaneous temperature distribution for 2 m square diesel pool fire.**

gradually decreases to 700 K in the plume region. A flame height of around 2*D* to 2.5*D* is observed.

*4.1.3. Adiabatic Surface Temperature and Heat Flux Onto the Cask* Plate thermometers attached to the cask are used to obtain the surface temperature and determine the incident heat flux. The plate thermometers record the transient temperature rise. Figure 4 shows the plate thermometer readings obtained for the 30 min of fire. All the plate thermometers indicated reasonably the same temperatures. Temperatures recorded by the plate thermometers in the core region of the pool fire reveals a steady-state temperature of 1100 K.

Adiabatic surface temperature (AST) is an apparent surface temperature of a perfectly insulated surface exposed to the same thermal conditions as that of a real surface under consideration. The advantage of using the AST is that it is an effective temperature boundary condition that represents a combination of radiation and convection boundary conditions. From the average of the temperature distribution obtained from the four plate thermometers, the AST is determined by using Eq. (4).

Figure 5 shows the AST and incident heat flux onto a cask in a 2 m square diesel pool fire. Heat flux from the fire to the plate thermometer is determined from the thermal capacitance of the plate thermometers. The heat flux onto the cask initially increases as the fire grows and reaches a steady mass burning rate. It is quite evident from Fig. 5 that the net heat flux onto the cask decreases as the tem-

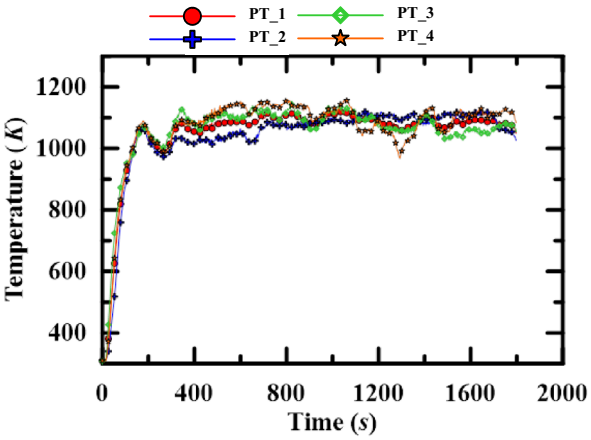


**Figure 4. Temperature distribution obtained by plate thermometers in 2 m diesel square pool fire.**

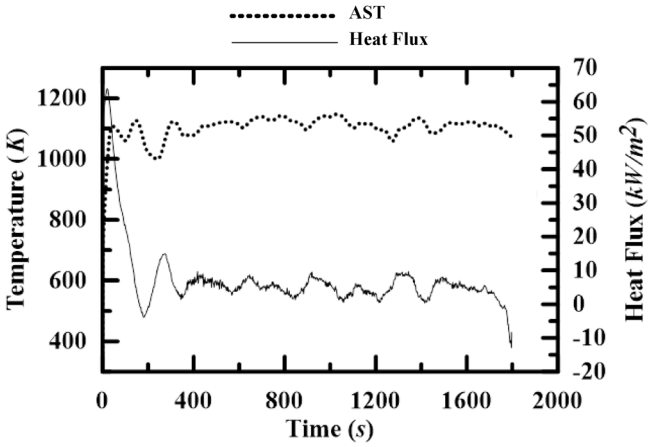


**Figure 5. Adiabatic surface temperature (AST) and Heat flux obtained from plate thermometers for 2 m diesel square pool fire.**

perature of the cask increases. When the temperature of the plate thermometer reaches close to the flame temperature, the net heat flux becomes almost zero.

The AST for a 2 m square diesel pool fire is found to be 1120 K. However, the adiabatic surface temperature reported for 1 m circular pool fire is 1100 K [16] and for 4 m square diesel pool fire is 1300 K [24]. Similarly, the peak heat flux obtained for the 2 m square diesel pool fire is about 60 kW/m$^2$. While the heat flux reported for 1 m circular pool fire is about 60 to 70 kW/m$^2$ [16], for 4 m square diesel pool fire is 115 kW/m$^2$ [24] and for 6 m diesel pool fire is 145 kW/m$^2$ [23]. It is thus evident that the values obtained for the mass burning rate, the

adiabatic surface temperature, and the heat flux to the cask are lower than that expected for a 2 m diesel square pool fire.

During the experiment, it is observed that the water surrounding the pool fire had started to boil as shown in Fig. 6. This phenomenon led the authors to hypothesize that the entrainment of surrounding water changes the dynamics of the pool fire resulting in the decrease of mass burning rate, the adiabatic surface temperature, and the heat flux onto the cask.

*4.1.4. Mass Burning Rate of 2 m Square Diesel Pool Fire without Water Surrounding the Pan* To corroborate the fact that water surrounding the pool fire indeed decreases the mass burning rate, the experiment was performed to determine the mass burning rate of the 2 m square diesel pool fire without water surrounding the pan. The pan filled with diesel fuel was burnt in 30 min and the overall mass burning rate is determined to be equivalent to 49.5 g/m$^2$s. Table 1 provides the evaluated average mass burning rate from the experimental investigations for the 2 m square diesel pool fire without water surrounding the pan.

## *4.2. Scaled-Down Experiments on 0.5 m Diesel Pool Fire*

To determine the effect of water surrounding the pool fire, small-scale 0.5 m diesel pool fire experiments are carried out. For the case of a pan not surrounded by water, the instantaneous mass loss rate is obtained by using the platform scale. For the case of a pan surrounded by water, the initial and final weight of diesel and water is obtained. With the duration of the experiment known, the mass-loss rate for diesel is determined.

*4.2.1. Mass Burning Rate of 0.5 m Diesel Pool Fire* Table 1 provides the experimentally measured mass loss rate of 0.5 m diesel pool fire for the three different cases.

The average mass loss rate for a 0.5 m simple diesel pool fire is 28.57 g/m$^2$s. For the pool fire case with water surrounding the pan, the mass loss rate was observed to decrease to 19.24 g/m$^2$s. In this case, an average of 2.8 kg of water is lost in 1500 s. Upon insulating the surrounding water with asbestos and cerablanc, the mass loss rate was observed to increase back to the simple pool fire case.

*4.2.2. Temperature Distribution 4.2.2.1. Pool Fire Not Surrounded by Water* K-type thermocouples are used to measure the centerline temperature distribution in the 0.5 m diesel pool fire. Figure 7a shows the temperature history of a 0.5 m diesel pool fire for the case with no water surrounding the pan. The temperatures obtained by thermocouples have been corrected for radiation using Eq. (5). The temperature indicated by the thermocouple TC_1, which is at the base of the pool fire is about 900 K. The temperature indicated by thermocouples TC_2 and TC_3 are higher, indicating the combustion zone. The temperatures obtained from the rest of the thermocouples indicate a decrease in temperature with an increase in height.

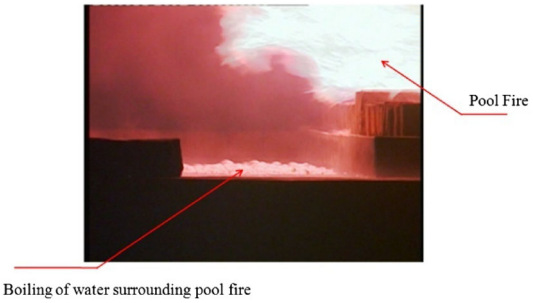


**Figure 6. Photograph depicting boiling of the water surrounding the diesel pool fire.**

Figure 7b shows the temperature contour obtained by averaging nearly 80 instantaneous thermal images of a pool fire. An emissivity value of 0.53, as obtained from the mass burning rate, is used as an input to the thermal camera. The temperature distribution indicates a core region of the constant temperature of 1000 K as observed for thermocouples TC_2 and TC_3. As the burnt and unburnt combustion gases move up due to buoyancy force, they get cooled by mixing up with ambient air, and hence the temperature decreases along with the height of the pool fire.

Figure 8 shows the comparison between the centerline temperature distribution for diesel pool fire of 0.5 m diameter and the centerline temperature distributions reported by McCaffrey [25] for natural gas and Koseki [26] for heptane pool fires. McCaffrey [25] made use of a square burner of side 0.3 m to produce a purely buoyant natural gas diffusion flame and different heat release rates were obtained by varying the gas flow rate. Koseki [26] determined the centerline temperature distribution for heptane pool fires of diameter 0.3 and 0.6 m. The heat release rate is represented by $Q = m'' A\Delta H_c$ where Q is the total heat release rate assuming perfect combustion (kW), A is the area of the pool fire ($m^2$) and $\Delta H_c$ is the heat of combustion (kJ/kg).

From the plot of variation in $\Delta T$ with $[Y/Q^{(2/5)}]^{\eta}$, McCaffrey concluded that the temperature rise is constant in the continuous flame zone, follows a -1 decay slope in the intermittent zone, and a -5/3 decay slope in the plume zone. Figure 8 indicates that the profile obtained for 0.5 m diesel pool fire matches well with that reported by McCaffery [25] and Koseki [26]. The measurements are in the flame as well as the intermittent regimes of the diesel pool fire. The quantitative differences between the present results and McCaffrey's data may be attributed to different flame heights, sooty flame of diesel, and assumed complete combustion. The flame height for natural gas ($3D$) is greater than diesel ($2.5D$) and hence there is a considerable change in the temperatures for diesel and natural gas pool fires at higher heights. Similar observations have been reported by Koseki [26] for heptane pool fires.

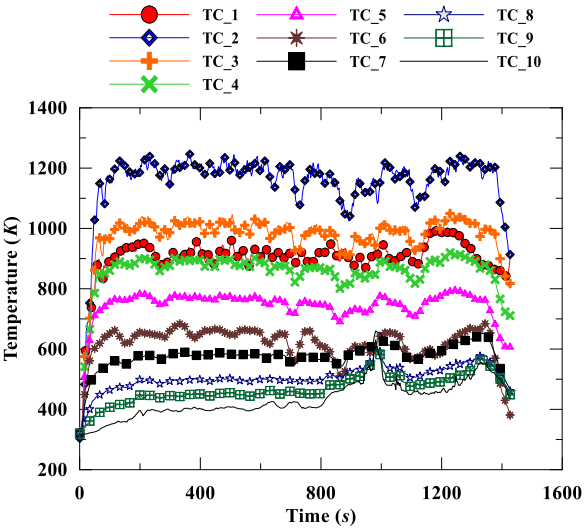


(a) Temperature distribution obtained from thermocouple

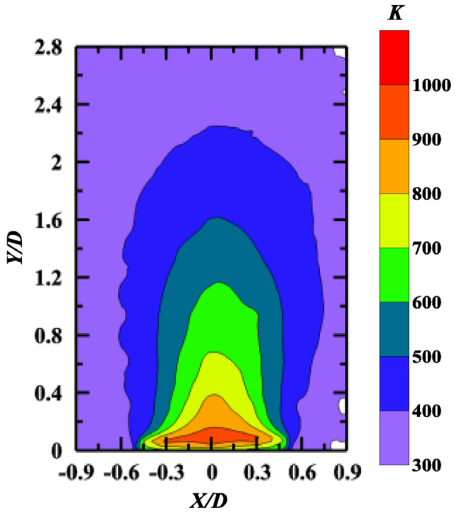


(b) Temperature distribution obtained using thermal camera

**Figure 7. Temperature distribution obtained using thermocouples and thermal camera for 0.5 m diameter diesel pool fire.**

*4.2.3. Pool Fire Surrounded by Water* For the pool fire case with water surrounding the pan, the temperature history is measured at the same locations. Figure 9a–c show the difference in the instantaneous temperature distribution obtained by the corresponding thermocouples for the two cases. From Fig. 9a, it can be observed that the average difference in the first three thermocouples is about 100 to 120 °C. Similarly, from Fig. 9b and c, it can be observed that the average dif-

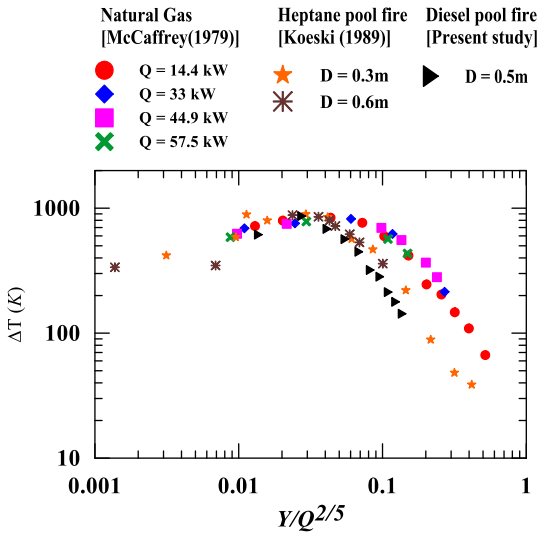


**Figure 8. Comparison of centerline temperature of diesel pool fire of 0.5 m diameter with that reported by McCafrey [25] and Koseki [26].**

ference is about 50 to 80 °C for thermocouples 4 to 6 and about 30 to 50 °C for the rest of the thermocouples. The difference in temperature for the two cases can be attributed to the entrainment of the water in the form of water vapor resulting in a decrease in the temperature of the pool fire. However, the difference in the temperature for thermocouples 6 to 10 is small. This small difference might be due to the completion of combustion beyond the water vapor entrainment zone and mixing due to turbulence. Figure 9d shows the comparison of the time-averaged centerline temperature distribution measured by thermocouples for both cases. It is observed that the average temperature has dropped by 100 °C for the thermocouples in the combustion zone. The temperature difference is found to decrease along with the height of the pool fire towards the plume region.

Figure 10 shows the temperature distribution in the water surrounding the pan. For the thermocouple located at a depth of 20 mm (TC_1w) from the top surface of the water, the temperature keeps increasing. At the end of the experiment, the temperature measured by that thermocouple almost reaches boiling point indicating that some amount of water on the surface has evaporated with boiling at the surface. The temperature measured by the other thermocouples (TC_2w to TC_5w), all located at a depth of 75 mm, show a gradual increase in temperature indicating a bulk increase of 5 °C.

From the above set of experiments, it can be observed that there is a 32.5% decrement in the mass loss rate due to water surrounding the 0.5 m diesel pool fire. It is also observed that the water surrounding the pool fire starts boiling/vaporizing. The decrease in the mass-loss rate is thus attributed to this interaction between the pool fire and water. The water vapor is entrained into the pool fire along with the surrounding air and this changes the dynamics of the pool fire

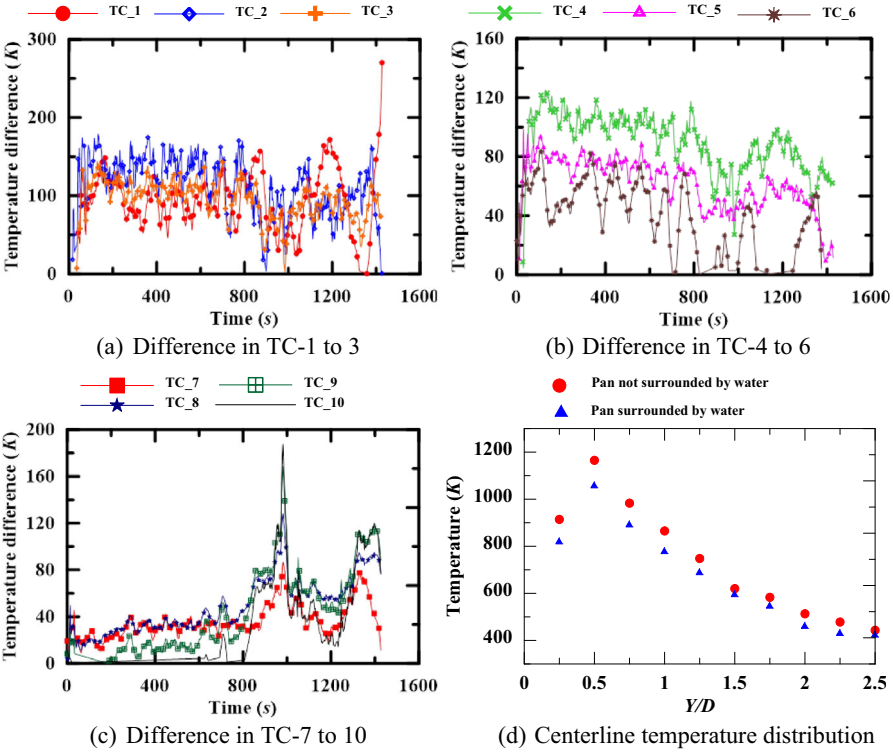


**Figure 9. Difference in temperature measured by thermocouples for 0.5 m diameter diesel pool fire with and without water surrounding the pan.**

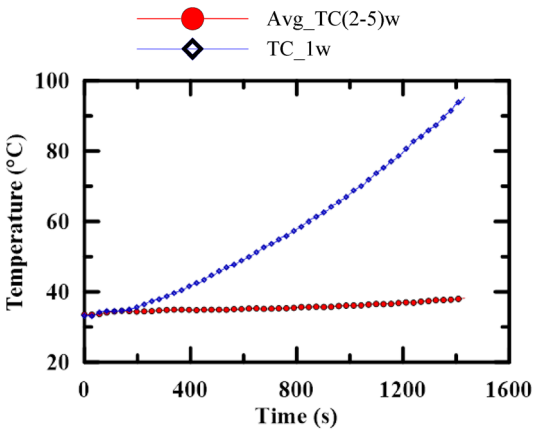


**Figure 10. Temperature distribution in the water surrounding the pan.**

resulting in lower heat feedback. Richard et al. [27] have determined the chemical and physical effects of water vapor addition on diffusion flames. They observed that adding water vapor affects both physical phenomena and chemical reactions by inhibiting the soot formation and shifting of CO to $CO_2$ formation. They noted that the cooling effect of water vapor and the subsequent decrease in temperature results in a decrease in the net heat feedback. The effect of water vapor on turbulent flames is the large-scale pool fire experiments conducted in Sandia National Laboratories (SNL) was demonstrated by Luketa and Blanchat [12]. They observed that smoke production in the SNL test was lesser than the Montoir experiments conducted by Nedelka et al. [28] and attributed it to the fact that the Montoir tests were conducted on land whereas for the SNL test the LNG was spilled over water. They cited various works to explain that the addition of water vapor from the substrate might be a plausible explanation for the discrepancy seen between the SNL and Montoir tests.

With the mass loss rate of water being 1.86 g/s (2.8 kg in 1500 s) in the present work, the amount of water present in the system is minimal. The decrease in temperature by the stated 100 °C is not only due to the evaporated water. This may be proved by evaluating the insignificant rate of heat removal by water vapors compared to the large heat release rate of fire with and without water around it. The interaction between the flame and the entrained water vapor is primarily in the core region of the flame as water vapor is entrained along with the ambient air in this region. When the products of combustion are primarily water vapor, any further addition of water vapor through the evaporation process tends to change the equilibrium towards the reactants side, resulting in a slightly endothermic reaction. Several other studies have demonstrated the physical and chemical effects of water addition on small-scale diffusion flames. For a methane counterflow diffusion flame, Zhang et al. [29] observed that the addition of water vapor either on the oxidizer or fuel side resulted in delayed soot nucleation and a significant reduction in the soot volume fraction due to OH interference with soot inception. To determine if addition of water into diffusion flame has any chemical effect, Atreya et al. [30] introduced water in either liquid or vapor form into the oxidizer stream. They observed that for a 30% $O_2$ oxidizer stream, water in the form of liquid droplets decreases CO and increases $CO_2$ production. Rao and Bardon [31] obtained similar results for hydrocarbon emulsions. Xu et al. [32] performed experimental and numerical studies to isolate the relative importance of the chemical, thermal, transport, and radiative effects of water addition in laminar coflow syngas diffusion flames. They showed that the overall effect of replacing $N_2$ in oxidizer with water is the decrease in the centerline temperature. Liu et al. [33] numerically investigated the effect of adding water vapor to the oxidizer stream on flame properties and soot formation in a laminar coflow ethylene/air diffusion flame. They demonstrated that addition of water vapor to the oxidizer stream significantly reduces the flame temperature and soot loading. These studies clearly demonstrate that water addition has both physical and chemical effects that can change the dynamics of the combustion processes of diffusion flames. The water vapor behaves as a diluent and acts as a heat sink by absorbing a part of the combustion energy [27]. However, with the amount of energy absorbed by water

being minimal, the authors believe that the reduction in temperature and mass loss rate is due to the effect of water on the flame chemistry. In general, it can be speculated that the addition of water increases the combustion efficiency resulting in a decrease in the soot volume fraction and hence emissivity of the flame. As no measurement of species distribution or soot volume fraction has been performed, it is difficult to explain the evolutions seen in the experiments and the interpretation can only be of qualitative and speculative nature.

The authors thus believe that a similar phenomenon is observed in pool fires due to the water surrounding the pan. The experimentally obtained mass burning rate of 2 m diesel pool fire surrounded by water (35 $g/m^2s$) is significantly lower than the expected mass burning rate (50.06 $g/m^2s$). This measured burning rate is lower by 30.1%. Interestingly, this deviation matches with the scaled-down experiments of 0.5 m pool fire. Emissivity values for the 2 m diesel pool fire surrounded by water decrease from 0.95 to 0.65. This decrease in the emissivity is the prime cause for the corresponding decrease in the heat flux to the packages to be tested in a pool fire.

## 5. Conclusions

Experiments were performed to measure the adiabatic surface temperature and heat flux onto a miniaturized cask in a 2 m square diesel pool fire. It was observed that the obtained values of the mass burning rate of the pool fire, the adiabatic surface temperature, and the heat flux to the cask were lower than what was expected for 2 m diesel square pool fire. The observation that the water surrounding the pool fire had started to boil led to the hypothesis that the interaction between the pool fire and the surrounding water changes the pool fire dynamics.

Experiments were then conducted on 0.5 m diesel pool fire to confirm the hypothesis. The mass-loss rate of diesel pool fire surrounded by water was found to be approximately 32% lesser than the mass-loss rate for the open pool fire scenario. Transient measurement of temperature reveals a drop of 100°C in the core region of the 0.5 m pool fire surrounded by water.

Thus, the decrease in the mass-loss rate of the pool fire, lower adiabatic surface temperature, and heat flux can be attributed to the interaction of pool fire with the surrounding water. The entrained water vapor acts as a heat sink and absorbs a part of the combustion energy. It is speculated that the addition of water vapor changes the flame chemistry resulting in a decrease in the amount of soot formation. This results in a decrease in the overall emissivity and hence the net radiative heat feedback thereby decreasing the mass burning rate.

It is thus suggested that the pool fire testing of casks be carried out by ensuring no interaction between water and the pool fire. This will ensure that the cask is exposed to the right temperature and emissivity and hence heat flux.

## Acknowledgements

The authors thank Mr. Rahul Shirsat for his help in building the experimental setup.

## Declarations

**Conflict of interest** All authors declare that they have no conflict of interest.

## References

1. IAEA Safety Standards Series No. TS-R-1, (2005) Regulations for the Safe Transport of Radioactive Material
2. Uncapher, W.L. and Hohnstreiter, G.F., (1995) *Radioactive material package testing capabilities at Sandia National Laboratories* (No. SAND–95–0202C; CONF-951203–26). Sandia National Labs., Albuquerque, NM (United States)
3. Van Sant, J.H., Carlson, R.W., Fischer, L.E. and Hovingh, J., (1993) A Guide for Thermal Testing Transport Packages for Radioactive Material—Hypothetical Accident Conditions. *Lawrence Livermore National Laboratory, Livermore, CA, UCRL-ID-110445*
4. Koski JA, Gritzo LA, Kent LA, Wix SD (1996) Actively cooled calorimeter measurements and environment characterization in a large pool fire. Fire Mater 20(2):69–78
5. Bainbridge BL, Keltner NR (1988) Heat transfer to large objects in large pool fires. J Hazard Mater 20:21–40
6. Kramer MA, Greiner M, Koski JA, Lopez C, Suo-Anttila A (2003) Measurements of heat transfer to a massive cylindrical calorimeter engulfed in a circular pool fire. J Heat Transfer 125(1):110–117
7. Longenbaugh, R.S., Sanchez, L.C. and Mahoney, A.R., (1990) *Thermal response of a small scale cask-like test article to three different high temperature environments. Sandia National Laboratories Report to Federal Rail Administration*. DOT/FRA/ORD-90/01
8. Koski JA, Gill W, Gritzo LA, Kent LA, Wix SD (1995) Characterization of indoor and outdoor pool fires with active calorimetry. ASME-Publications-HTD 304:79–88
9. Gregory JJ, Keltner NR, Mata R (1989) Thermal measurements in large pool fires. J Heat Transfer 111(2):446–454
10. del Valle, M.A., Kramer, M.A., Lopez, C., Suo-Anttila, A. and Greiner, M., (2007) October. Temperature response of a rail-cask-size pipe calorimeter in large scale pool fires. In *proceedings of the 15th International Symposium on the Packaging and Transportation of Radioactive Materials* (pp. 21–26)
11. Sudheer S, Wehrstedt KD, Prabhu SV (2016) Heat transfer to bodies engulfed in di-tert-butyl peroxide pool fires-Numerical simulations. J Loss Prev Process Ind 44:204–211
12. Luketa A, Blanchat T (2015) The phoenix series large-scale methane gas burner experiments and liquid methane pool fires experiments on water. Combust Flame 162(12):4497–4513
13. ASTM Standard E 2230 (2002) Standard Practice for Thermal Qualification of Type B packages for Radioactive Material.ASTM International, West Conshohocken, PA

14. Nakos, J.T. and Keltner, N.R., 1989 *The radiative-convective partitioning of heat transfer to objects in large pool fires* (No. SAND-89–0360C; CONF-890819–5). Sandia National Labs., Albuquerque, NM (USA)
15. Sudheer S, Prabhu SV (2012) Measurement of flame emissivity of hydrocarbon pool fires. Fire Technol 48(2):183–217
16. Sudheer S, Prabhu SV (2013) Heat transfer in vertical casks engulfed in open pool fires. J Fire Sci 31(6):541–562
17. Babrauskas V (1983) Estimating large pool fire burning rates. Fire Technol 19(4):251–261
18. Wickström U (2011) The adiabatic surface temperature and the plate thermometer. Fire Safety Science 10:1001–1011
19. Silvani X, Morandini F (2009) Fire spread experiments in the field: temperature and heat fluxes measurements. Fire Saf J 44(2):279–285
20. Bergman TL, Incropera FP, DeWitt DP, Lavine AS (2011) Fundamentals of heat and mass transfer. John Wiley & Sons,
21. Moffat RJ (1985) Using uncertainty analysis in the planning of an experiment. J Fluids Eng 107:173–178
22. Rew PJ, Hulbert WG, Deaves DM (1997) Modelling of thermal radiation from external hydrocarbon pool fires. Process Saf Environ Prot 75(2):81–89
23. Muñoz M, Arnaldos J, Casal J, Planas E (2004) Analysis of the geometric and radiative characteristics of hydrocarbon pool fires. Combust Flame 139(3):263–277
24. Sudheer S, Kumar L, Manjunath BS, Pasi A, Meenakshi G, Prabhu SV (2013) Fire safety distances for open pool fires. Infrared Phys Technol 61:265–273
25. McCaffrey, B.J., (1979) *Purely buoyant diffusion flames: some experimental results*. Center for Fire Research, NBS
26. Koseki H (1989) Combustion properties of large liquid pool fires. Fire Technol 25(3):241–255
27. Richard J, Garo JP, Souil JM, Vantelon JP, Knorre VG (2003) Chemical and physical effects of water vapor addition on diffusion flames. Fire Saf J 38(6):569–587
28. Nedelka, D., Moorhouse, J. and Tucker, R.F., (1989)*The Montoir 35m diameter LNG pool fire experiments*. Midlands Research Station
29. Zhang C, Atreya A, Lee K (1992) January Sooting structure of methane counterflow diffusion flames with preheated reactants and dilution by products of combustion. Symposium International on Combustion 24(1):1049–1057
30. Atreya A, Crompton TODD, Suh JAEIL (2000) A study of the chemical and physical mechanisms of fire suppression by water. Fire Safety Science 6:493–504
31. Rao VK, Bardon MF (1984) The effect of water on gas phase soot formation in laminar diffusion flames. Combust Flame 55(1):73–78
32. Xu H, Liu F, Sun S, Zhao Y, Meng S, Tang W (2017) Effects of H2O and CO2 diluted oxidizer on the structure and shape of laminar coflow syngas diffusion flames. Combust Flame 177:67–78
33. Liu F, Consalvi JL, Fuentes A (2014) Effects of water vapor addition to the air stream on soot formation and flame properties in a laminar coflow ethylene/air diffusion flame. Combust Flame 161(7):1724–1734